Fang *et al. Chem Synth* 2024;4:51
DOI: 10.20517/cs.2024.06

Chemical Synthesis

Research Article

Open Access

Fluorescence detection and effective adsorption of trace Pb(II) based on nanofibrous metal-organic gel

Yu Fang, Kechun Yu, Guojian Ren*, Cong Wang, Qi Zhou, Guang Che, Meiling Li, Qinhe Pan*

Key Laboratory of Advanced Materials of Tropical Island Resources, Ministry of Education, School of Chemistry and Chemical Engineering, Hainan University, Haikou 570228, Hainan, China.

***Correspondence to:** Prof. Guojian Ren, Prof. Qinhe Pan, Key Laboratory of Advanced Materials of Tropical Island Resources, Ministry of Education, School of Chemistry and Chemical Engineering, Hainan University, 58 Renmin Avenue, Haikou 570228, Hainan, China. E-mail: rgj860508@163.com; panqinhe@163.com

How to cite this article: Fang Y, Yu K, Ren G, Wang C, Zhou Q, Che G, Li M, Pan Q. Fluorescence detection and effective adsorption of trace Pb(II) based on nanofibrous metal-organic gel. *Chem Synth* 2024;4:51. https://dx.doi.org/10.20517/cs.2024.06

Received: 16 Jan 2024 **First Decision:** 29 Mar 2024 **Revised:** 26 Apr 2024 **Accepted:** 16 May 2024 **Published:** 3 Sep 2024

Academic Editor: Guangshan Zhu **Copy Editor:** Pei-Yun Wang **Production Editor:** Pei-Yun Wang

Abstract

Water pollution has become a global environmental problem, such as that caused by Pb(II). Therefore, there is an urgent need to develop multifunctional materials for Pb(II) monitoring and removal. Yet, developing bifunctional materials for sensitive detection and efficient removal of Pb(II) remain challenging. Here, a metal-organic gel (HNU-G4) was constructed for sensible responsive detection and efficient adsorption of Pb(II). The dry gel was obtained through the freeze-dried process and can be used for the Pb(II) detection via fluorescence quenching; the lowest limit of detection for Pb(II) is 0.766 ppb. Furthermore, HNU-G4 has an effective maximum adsorption capacity of 480.00 $mg \cdot g^{-1}$ for Pb(II) in water. Additionally, the gel demonstrates excellent recoverability and interference resistance, which can be used in the detection and recovery of actual reclaimed water samples to prevent secondary contamination. This study developed a bifunctional gel material for sensitive detection and effective removal of Pb(II) from water, providing a suggested strategy to tackle the heavy metal contamination problem.

Keywords: Metal-organic gel, Pb(II), adsorption, detection, reclaimed water

INTRODUCTION

With the rapid development of modern industry and the increase in human economic activities, heavy

metal pollution has gradually become a global environmental issue[1,2]. Among the hazardous pollutants, heavy metal Pb(II) ions have received widespread attention due to their hazardous nature. The presence of Pb(II) not only threatens natural ecosystems but also poses risks to human health[3]. As it accumulates in the environment and human body, the toxic effects will affect the central nervous, digestive, reproductive, and immune systems[4]. To solve the critical issue, developing environmentally friendly materials for detecting and adsorbing heavy metal Pb(II) from water has become quite urgent.

Aimed at highly efficient detection of Pb(II), functional materials, including mesoporous nanocomposites[5], metal/covalent organic frameworks (MOFs/COFs)[6,7], and magnetic nanoparticles[8], have been developed. As a class of multifunctional materials, metal-organic gels (MOGs) have attracted widespread interest due to their excellent stabilities and unique structure. They are gel-like materials constructed through coordination between metal ions and organic molecules and non-covalent interactions including π-π stacking, hydrogen bonding, and van der Waals forces[9], which possess highly tunable structures, adjustable porosity, open active sites[10], and functional groups[11]. Benefiting from these characteristics, MOGs show a wide range of possibilities for application in the areas of catalysis[12], adsorption[13], separation[14], sensing[15], *etc.*

As for Pb(II) adsorption, the -NH_2 group and uncoordinated N atom were adopted to improve the adsorbed amount of MOGs[16]. For example, Huang *et al.* used Zn to prepare an excellent amino MOF adsorbent for removing lead, mercury, and arsenic from water[17]. Separately, Yin *et al.* developed an effective method for removing Pb(II) by combining amino-functionalized MOFs with ceramic membrane ultrafiltration[18]. Nonetheless, the low concentration Pb(II) adsorption remains a tough problem. In addition, although the MOGs for Pb(II) adsorption have been developed, the fluorescence sensing was less explored, such as the new multifunctional gel developed by Kumar *et al.* and Varaprasad *et al.*[19,20]. Detecting the content of Pb(II) and adsorbing low concentration Pb(II) present great challenges.

By introducing functional groups and modulating the structure of MOGs, the fluorescence detection and low concentration Pb(II) adsorption could be achieved. This work adopted the organic ligand 2,2'-(1,4-phenylene)bis(1H-benzo[d]imidazole-5-carboxylic acid) (H_2L_1) which contains the fluorescence and coordination groups. Synthesis of metal organogels, fluorescence sensing detection and adsorption of Pb(II) were demonstrated in Scheme 1. In the ligand, the benzimidazole can serve as a fluorescence group, and the -COOH and N-H groups can serve as chelating groups for the high adsorption of Pb(II). Through the assembly of H_2L_1 and Zr^{4+}, a MOG (HNU-G4) with fibrous morphology was synthesized. It should be mentioned that the minimum detection limit is 0.766 ppb, much lower than the maximum Pb(II) ion level in drinking water set by the World Health Organization (WHO)[3,4]. Furthermore, the adsorption amount of HNU-G4 for Pb(II) can reach 480.00 $mg \cdot g^{-1}$, with a removal rate of 99.98% in the trace concentration Pb(II) environment. This study provides feasible methods to address Pb(II) pollution and offers robust support and assurance for environmental protection and human health.

EXPERIMENTAL

The detailed materials and methods in the experiment were listed in the Supplementary Materials.

Synthesis of H_2L_1 and HNU-G4

The synthesis path for H_2L_1 is shown in Supplementary Figure 1A. Terephthalaldehyde (2.50 g, 0.019 mol) was added to 45 mL $NaHSO_3$ (40% wt.) solution and sonicated for 2 h, and then 3,4-diaminobenzoic acid (5.60 g, 0.037 mol) was dispersed in 100 mL ethanol and added in the solution above slowly. The resulting mixed solution was stirred at 25 °C for 30 min followed by reflux for 5 h. In the next step, the filtered solid

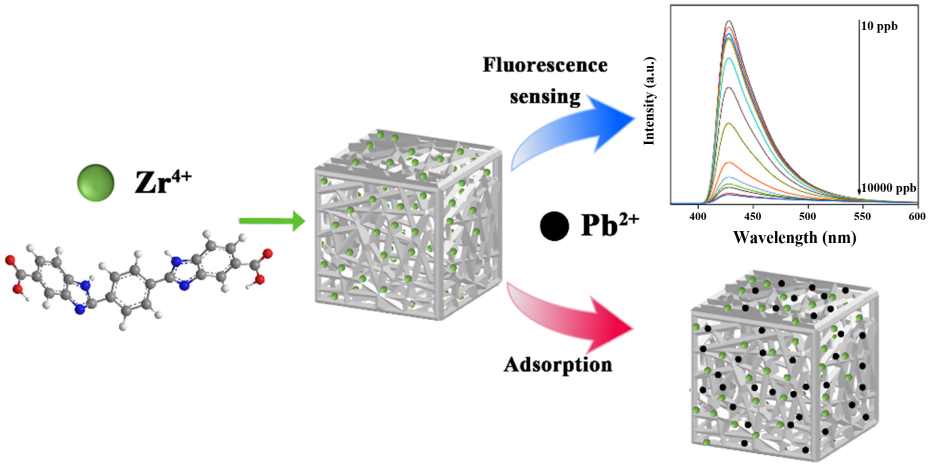

Scheme 1. Synthesis of metal-organic gel, fluorescence sensing detection and adsorption of Pb(II).

was washed by immersion in water and ethanol after the reaction product was cooled to 25 °C and finally recrystallized in a mixed solution [H_2O:N,N-Dimethylformamide (DMF) = 1:9, v/v] to obtain H_2L_1. The proton magnetic resonance (^{1}H NMR) or carbon-13 nuclear magnetic resonance (^{13}C NMR) data of H_2L_1 are shown in Supplementary Figures 2 and 3.

$ZrCl_4$ (0.05 mM), H_2L_1 (20 mg) and 1.5 mL DMF were placed in a 10 mL glass vial. The mixture was heated at 368 K for three days. The vials were cooled naturally to obtain a yellow wet gel, followed by freeze-drying for 24 h after washing and soaking with ethanol three times to obtain a dry gel[21]. The synthesis path for HNU-G4 is shown in Supplementary Figure 1B.

Fluorescence sensing of HNU-G4 on Pb(II)

Fluorescence measurement of Pb(II) detected by HNU-G4 was performed using the following procedure. The HNU-G4 dry gel was ground to a homogeneous powder, dispersed in water, and then sonicated for 5 min to prepare a 1 mg·mL^{-1} suspension. The fluorescence response of HNU-G4 to Pb(II) at the same concentration and different pH was verified, and then the fluorescence response of HNU-G4 to varying concentrations of Pb(II) was performed. Pb(II) solutions of 0-10 ppm were added to 5 mL of HNU-G4 suspension respectively, mixed well, and then the fluorescence spectra of these samples were measured. The fluorescence responses of HNU-G4 to various metal ions were examined to better understand its effectiveness in detecting Pb(II). The selectivity of HNU-G4 was evaluated by adding various common metal ions [Pb(II), Ca(II), Co(II), Zn(II), Mg(II), Ni(II), K(I), and Na(I)] into the suspension. The common metal ions were mixed, and the corresponding interference of HNU-G4 on Pb(II) was verified by fluorescence response.

Batch adsorption experiments

The test solution in the experiment is prepared with $Pb(NO_3)_2$. The impact of pH on adsorption was examined with Pb(II) solutions of pH = 1.0-7.0, and equilibrating pH with 0.1 mol·L^{-1} HCl and NaOH. HNU-G4 (3.0 mg) and Pb(II) solution (20 mg·g^{-1}, 90 mL) were mixed well and tested at different time intervals, and the residual Pb(II) content was also determined to study the adsorption kinetics. Pb(II) solutions (90 mL) with concentrations ranging from 5.0 to 200.0 mg·g^{-1} were added with HNU-G4 (3.0 mg), and the residual Pb(II) content was measured to obtain adsorption isotherms. The equilibrium adsorption capacity (Q_e, mg·g^{-1})[22] and time-dependent adsorption capacity (Q_t, mg·g^{-1})[23,24] of HNU-G4 for Pb(II) are computed by

$$Q_t = \frac{(C_0 - C_t)\ V}{m} \quad (1)$$

$$Q_e = \frac{(C_0 - C_e)\ V}{m} \quad (2)$$

The Pb(II) removal rate from the solution is obtained by[25-27]

$$R = \frac{C_0 - C_e}{C_0} \times 100\% \quad (3)$$

where C_0 and C_t denote the initial concentration and the equilibrium concentration of Pb(II) (mg·L^{-1}) at a certain time; C_e and Q_e are the concentration and the amount of adsorption in equilibrium. V is the volume of the adsorbed environmental solution (L). m denotes the weight of **HNU-G4** (g). R is the recovery rate.

Solutions containing eight metal ions [Pb(II), Ca(II), Co(II), Zn(II), Mg(II), Ni(II), K(I), and Na(I)] were used to verify the adsorption of competing coexisting ions at a solution of 20 mg·L^{-1}. Briefly, HNU-G4 (3.0 mg) and 90 mL of mixed metal ion solution were mixed well and shaken in a shaker at 25 °C for 150 min. Centrifugal filtering removed the adsorbent, and inductively coupled plasma (ICP)-optical emission spectrometry (OES) determined the amounts of different metal ions in the solution. The selectivity of HNU-G4 adsorption on Pb(II) and the impact of other metal ions on the substance's ability to adsorb Pb(II) were both identified. The other seven single-ion solutions were combined with 20 mg·L^{-1} of Pb(II) in a 90 mL volume. Then, 3.0 mg of HNU-G4 was added, and the mixture was agitated for 150 min at 25 °C. When the adsorbents were removed, the concentrations of various common metal ions in the solution were examined by ICP to investigate interfering effect of other metal ion pairs during the adsorption of Pb(II) by HNU-G4.

Regeneration experiments

The HNU-G4 adsorbed with Pb(II) [HNU-G4-Pb(II)] was combined with a 0.1 mol·L^{-1} solution of HCl. The eluate was sampled and tested for Pb(II) levels after being shaken for 2 h. Deionized water and EtOH were used for cleaning; HNU-G4 was dried at 60 °C to obtain regenerated HNU-G4. During the cyclic experiment, the process was repeated for the second cycle, which was conducted for six cycles.

RESULTS AND DISCUSSION

Characterization analysis

The powder X-ray diffractometer (PXRD) pattern reveals that HNU-G4 is amorphous [Figure 1A][28,29]. In Figure 1B, stretching and bending vibrations of amino N-H were observed at 3,765 and 1,109 cm^{-1}, respectively. The peaks at 3,300-3,800 cm^{-1} were attributed to the stretching vibrations of -OH. Additionally, the peaks at 823 and 663 cm^{-1} were assigned to -C=N- and O-Zr, respectively. The thermogravimetric analysis (TGA) curve [Figure 1C] decreases significantly around 430 °C, which can be considered as the disruption of the internal structure of HNU-G4. A wet gel optical photo of HNU-G4 is shown in Supplementary Figure 4. From the scanning electron microscopy (SEM) image of the gel [Figure 1D], its surface shows a flower-like fiber structure with each fiber intertwined, which gives the gel a high specific surface area, and no clear crystalline phase is found. N_2 adsorption measurements were performed at 77 K to evaluate the porosity of HNU-G4 (Supplementary Figure 5, the illustration shows the aperture distribution). The Brunauer-Emmett-Teller (BET) surface areas determined from the N_2 adsorption isotherms were 4.341 m^2/g.

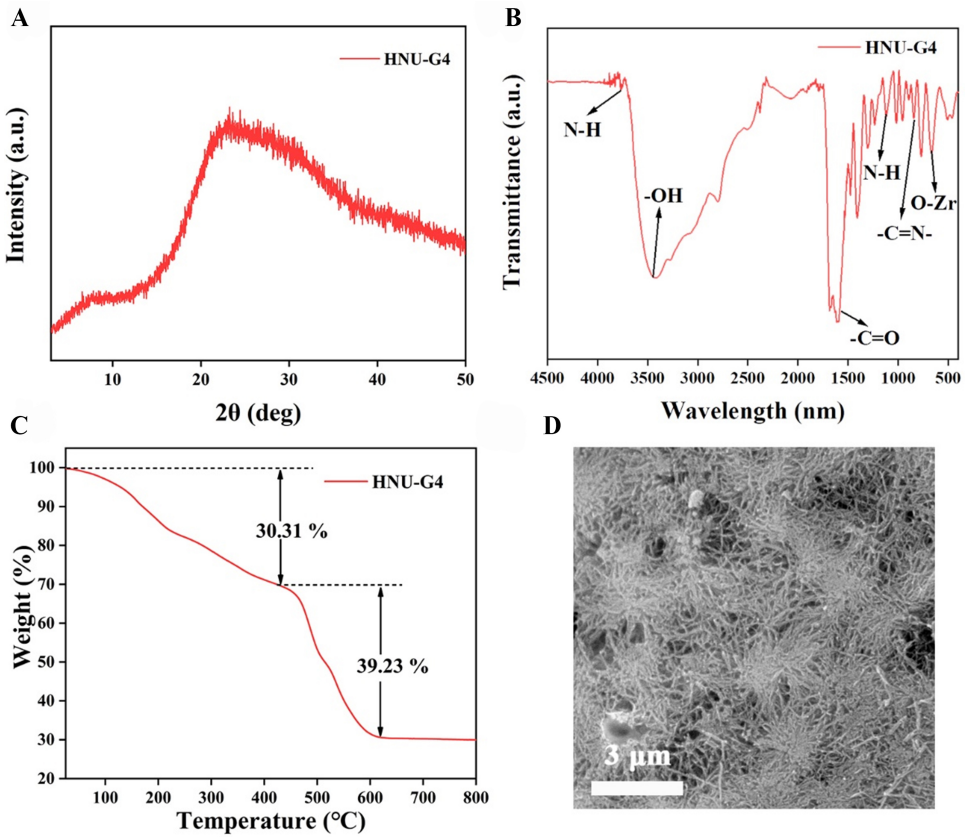

Figure 1. (A) The PXRD pattern of HNU-G4; (B) FT-IR spectrum of HNU-G4; (C) TG plot of HNU-G4; (D) SEM image of the dry gel HNU-G4. PXRD: Powder X-ray diffractometer; FT-IR: Fourier transform infrared spectrometer; TG: thermogravimetry; SEM: scanning electron microscopy.

Fluorescence sensing performance of HNU-G4 for Pb(II)

The emission spectrum of HNU-G4 in water was examined [Supplementary Figure 6], with an emission peak at 504 nm (λ_{ex} = 339 nm). Additionally, the fluorescence response of HNU-G4 to common metal ions in water was tested. The Ca(II), Co(II), Zn(II), Mg(II), Ni(II), K(I), Na(I) and Pb(II) ions were introduced into the HNU-G4 suspension. The results showed that only Pb(II) showed fluorescence quenching of HNU-G4, while the existence of other common metal ions did not significantly attenuate or enhance the fluorescence about HNU-G4 [Figure 2A and B]. The quenching efficiency was calculated by[29,30]

$$\frac{I_0\text{-}I}{I_0} \times 100\% \quad (4)$$

Where I_0 and I are the fluorescence intensity of HNU-G4 before and after mixing Pb(II). The fluorescence intensity of HNU-G4 was attenuated by up to 87.51% after the addition of Pb(II) [Figure 2B], while the quenching efficiency of other metal ions for HNU-G4 was less than 5%, and the results showed that the selectivity for detecting other metal ions was much lower than Pb(II). The sensitivity of HNU-G4 to Pb(II) was investigated by concentration-dependent experiments. Photoluminescence (PL) emission spectra [Figure 2C] showed that the fluorescence intensity of HNU-G4 decreased with increasing Pb(II) concentration, and when the Pb(II) concentration was small, the fluorescence intensity was almost linearly related to the analyte concentration [Figure 2C inset].

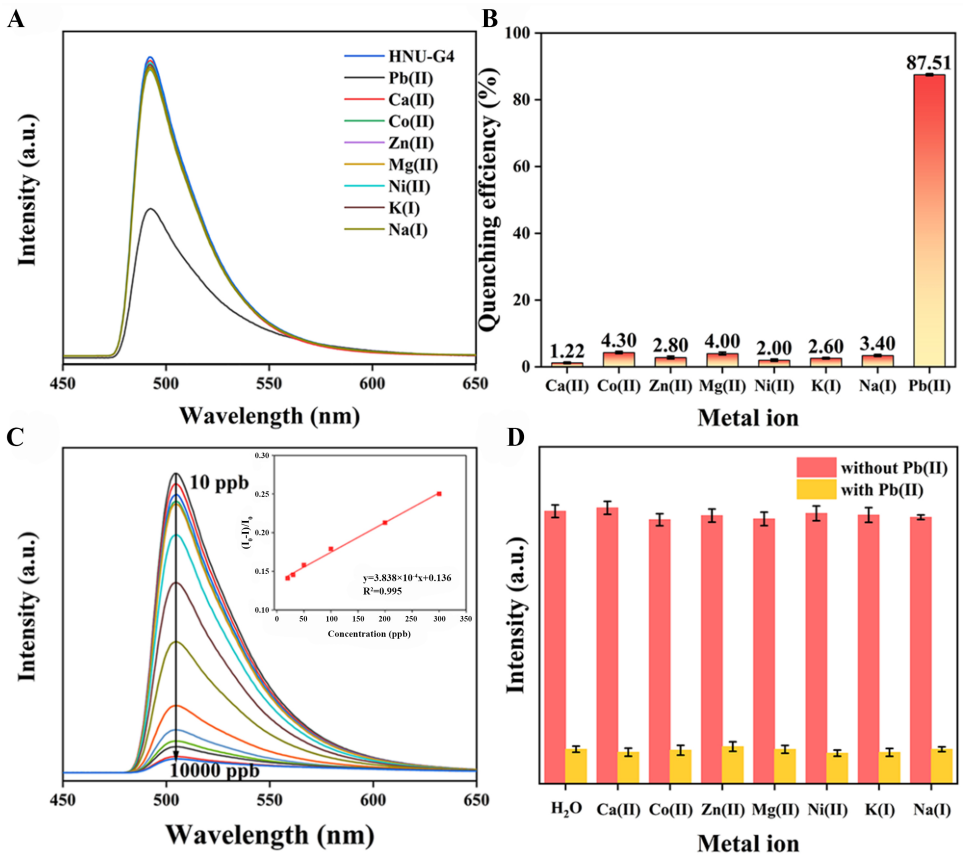

Figure 2. Fluorescence spectra (A) and quenching efficiencies (B) of HNU-G4 by various metal ions; (C) Fluorescence intensity of HNU-G4 in different concentrations of Pb(II) solutions, the illustration shows the linear relationship at low concentrations; (D) Fluorescence intensity of HNU-G4 in mixed solutions of other single metal ions and Pb(II).

In addition, the limit of detection (LOD) (3σ/K)[31-33] was calculated from the K value (K = 0.0383) and standard deviation (σ) of the fluorescence intensity of the blank samples. The calculated LOD was 0.766 ppb, comparable to or below the reported results [Table 1]. The low LOD can be attributed to chelation quenched fluorescence (CHQF) of HNU-G4. To verify the selectivity of HNU-G4 for Pb(II), further competition experiments were performed [Figure 2D], where the presence of other common metal ions did not interfere with the reactivity of HNU-G4 to Pb(II). These results reveal that HNU-G4 exhibits specificity in detecting Pb(II).

Effect of pH in structure and adsorption

Structural stability is a critical consideration for evaluating the application of MOGs, so that of HNU-G4 was investigated in acidic solutions. HNU-G4 was tested after immersing it in solutions with pH = 1.0-7.0 for 12 h. No significant peaks of disappearance or displacement were observed in its PXRD patterns [Supplementary Figure 7], indicating that the structure remained intact and exhibited good acid stability. The initial pH and interfering ions affect the adsorption of heavy metal ions by the gel. It has been reported that the charge on the gel surface and the form of metal ions existing in the solution are influenced by pH. The presence forms of Pb ions at different pH values are shown in Supplementary Figure 8A[41]; these ions are mainly present as Pb^{2+} and in a small amount of $Pb(OH)^{+}$ at pH = 1.0-6.0. The zeta potential of HNU-G4 at varied pH levels is shown in Supplementary Figure 8B; at pH = 5, it is negative, indicating a weak electrostatic interaction with Pb^{2+}. The adsorption of Pb(II) by HNU-G4 is shown in Figure 3, at diverse pH

Table 1. Comparison of adsorption capacity, detection methods and detection limits for HNU-G4 and other adsorbents

Adsorbents	Adsorption capacity ($mg \cdot g^{-1}$)	Detection method	LOD (ppb)	Ref.
BUC-77	425.00	Fluorescence	6.910	[34]
IIMB	118.00	FAAS	0.950	[35]
Triplochyton scleroxylon	298.00	Electrochemical	0.820	[36]
mesoporous adsorbent	184.32	UV-vis-NIR	0.110	[15]
PCM	204.34	UV-vis spectrophotometer	0.330	[37]
UiO-66-NHC(S)NHMe	391.00	Electrochemical	2.300	[38]
P(TA-MBA-GGQDs)/Ge DN gel	259.067	Naked-eye and fluorescence	0.052	[16]
Functional composite material	176.66	UV-vis	0.440	[39]
Flower-like NiO/rGO nanocomposite	70.00	SWASV	2.070	[40]
HNU-G4	480.00	Fluorescence	0.766	This work

LOD: Limit of detection; IIMB: ion-imprinted magnetic biocomposite; FAAS: flame atomic absorption spectrometry; UV-vis-NIR: ultraviolet–visible–near infrared spectroscopy; PCM: porous composite material; rGO: reduced graphene oxide; SWASV: square wave anodic stripping voltammetry.

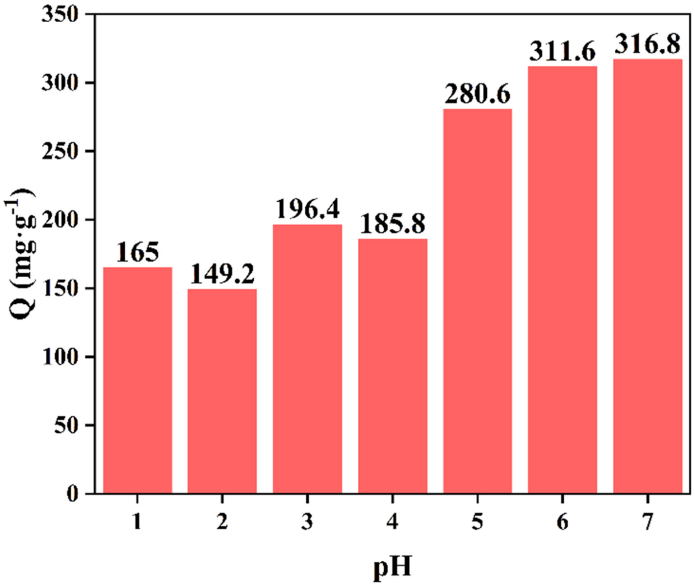

Figure 3. The adsorption capacity of Pb(II) at pH levels from 1 to 7, with an initial concentration of 50 $mg \cdot L^{-1}$.

values at 20 $mg \cdot L^{-1}$. In conjunction with literature reports[7,25], the subsequent kinetics and thermodynamics studies were conducted at pH = 5 as Pb(II) agglomerates under weakly acidic conditions.

Adsorption kinetics study

From 0 to 90 min, the adsorption curve reveals a sharp increase in adsorption. The adsorption curve slowly rises with time and reaches equilibrium after 120 min [Figure 4]. Modeling the adsorption kinetics allowed a more thorough investigation of the adsorption mechanism[42]. The parameters were provided in Supplementary Table 1, and the pseudo-first-order and pseudo-second-order kinetics were fitted independently [Figure 4]. With an adsorption of 298.26 $mg \cdot g^{-1}$, consistent with the experimental test data (296.88 $mg \cdot g^{-1}$), the experimental data are more in line with the pseudo-second-order model. The primary factor in the fit to the pseudo-second-order adsorption kinetics was the chemisorption adsorption curve during the adsorption process.

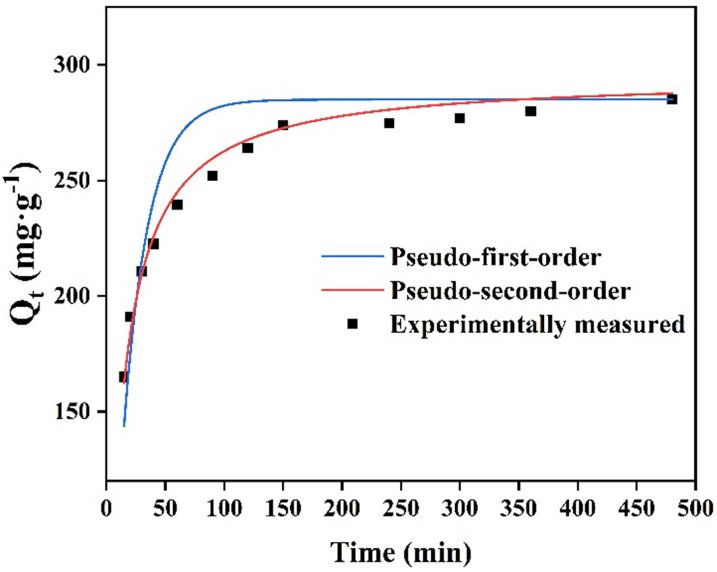

Figure 4. The pseudo-first-order (blue) and pseudo-second-order (red) models were used to fit the kinetic model of HNU-G4 adsorption Pb (II) process.

Adsorption isotherm study

The Langmuir and Freundlich isotherm models were applied to match the adsorption data, and the fitting results of the experimental data are shown in Figure 5 with detailed parameters in Supplementary Table 2. The experimental data matched the Langmuir model more closely. The estimated value of 468.00 mg·g^{-1} can be compared to the actual adsorption amount (468.05 mg·g^{-1}). Since HNU-G4 possesses a homogeneous distribution of adsorption sites, the adsorption method it uses to bind Pb(II) is monolayer adsorption. Compared to other adsorbents, the HNU-G4 developed in this study showed superior performance in adsorbing heavy metal ions. The adsorption performance of the different types of adsorbents is summarized in Table 1. In comparison, the HNU-G4 in this research performs better in adsorbing Pb (II).

Selectivity and reusability

Commonly used metal ions [Fe(III), Al(III), Zn(II), Cu(II)), Cd(II), Mn(II), Ca(II), Ni(II), Na(I), K(I)] were used to study the selectivity of Pb(II) adsorption by HNU-G4. In Figure 6A, the adsorption capacity of HNU-G4 on Pb(II) was stronger than that of other metal ions. To investigate the ability of HNU-G4 to adsorb Pb(II) in a multicomponent system, commonly used metal ions were selected as competing ions, and Supplementary Figure 9 displays the HNU-G4 ions in the competitive ion multicomponent system. The findings showed that Pb(II) was removed from the multicomponent system by HNU-G4 at a rate higher than that of other common metals and that other ions had no effect on Pb(II) adsorption by HNU-G4. As displayed in Figure 6B, the removal rate of Pb(II) by HNU-G4 did not decrease significantly after six cycles of experiments, and the removal efficiency remained above 98.68%.

Possible sensing and adsorption mechanisms

The element mapping of blank gel and the element atlas after immersion in Pb (II) solution are shown in Supplementary Figure 10, proving that Pb is adsorbed on HNU-G4. Based on these results, a possible mechanism of the fluorescence detection and adsorption by HNU-G4 on Pb(II) was proposed. Specifically, electron-rich carboxyl and N-H in organic ligands tend to donate electrons to the 6p-orbital of Pb(II) with vacant electrons[16]. Hence, the fluorescence sensing of Pb(II) by HNU-G4 was attributed to CHQF[16]. On the other hand, Pb(II) can be chelated with the reactive groups of the gel to effectively adsorb Pb(II)[43,44]. The peaks of Pb4f 7/2 and Pb4f 5/2 at 138.94 and 143.82 eV for HNU-G4-Pb(II) indicate that Pb(II) is

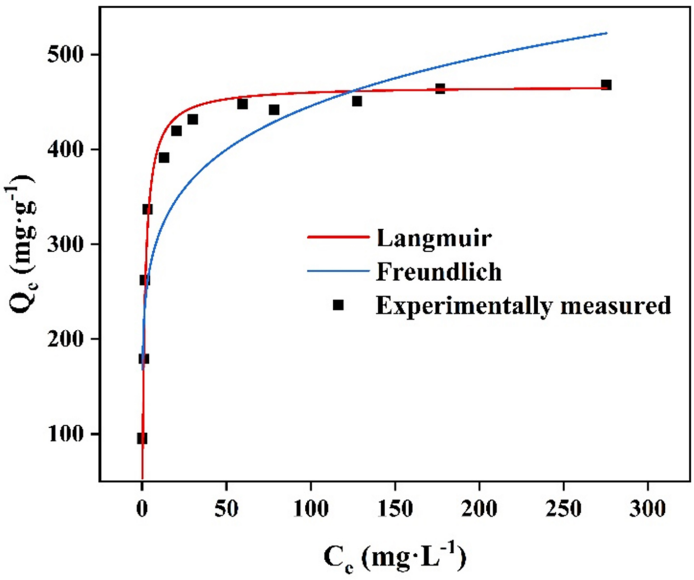

Figure 5. Adsorption isotherms for HNU-G4 were fitted nonlinearly, Langmuir (red) and Freundlich (blue).

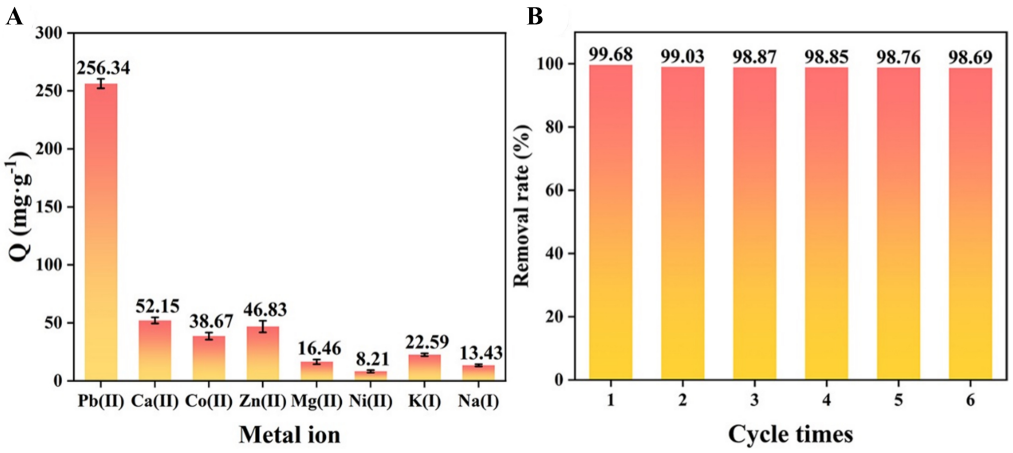

Figure 6. (A) Selectivity of HNU-G4 in mixed metal ion aqueous solution (the concentration of each ion is 20 mg·L^{-1}); (B) Recyclability of HNU-G4.

adsorbed on the material, as shown in the X-ray photoelectron spectroscopy (XPS) spectra [Figure 7A and B][8]. In Figure 7C, the C-OH, C=O and O-metal binding energies in the O1s spectrum of HNU-G4 change from 533.20, 531.98 and 531.14 eV to 533.15, 532.95 and 531.15 eV, respectively[35]. And the relative amount of the O-metal band increases from 30.96% to 42.78%, while the relative amounts of the C=O and C-OH bands decreased by 10.41% and 2.01%, respectively. Similarly, the peak of N1s slightly shifted after the adsorption of Pb(II) [Figure 7D], and the chemical shifts of N-metal, N-H and C=N were increased. The relative amount of N-metal rose from 29.10% to 40.20%, and the relative amounts of N-H and C=N decreased from 31.04% and 39.86% to 30.08% and 29.00%. The above results demonstrate that Pb(II) interacts with -N-H and -COOH.

Adsorption of Pb(II) to reclaimed water

The application with HNU-G4 in practice was verified through adsorption experiments using it on

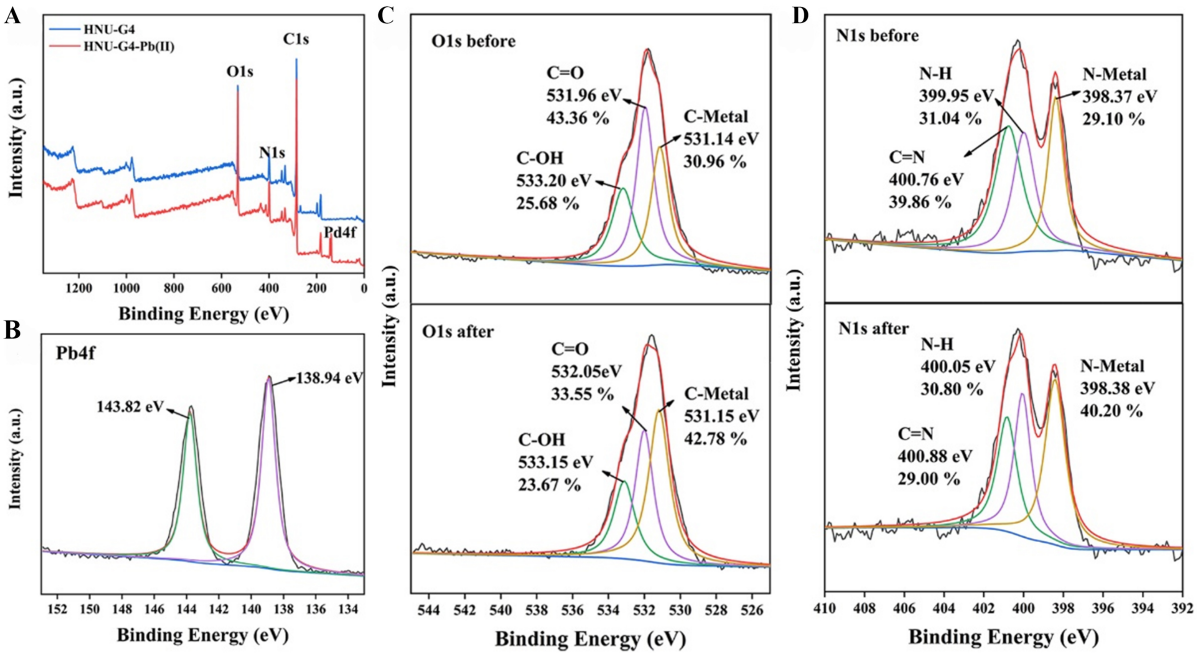

Figure 7. (A) The XPS spectra of HNU-G4 and HNU-G4-Pb(II), along with the high-resolution fitting outcomes for (B) Pb4f, (C) O1s, (D) N1s. XPS: X-ray photoelectron spectroscopy.

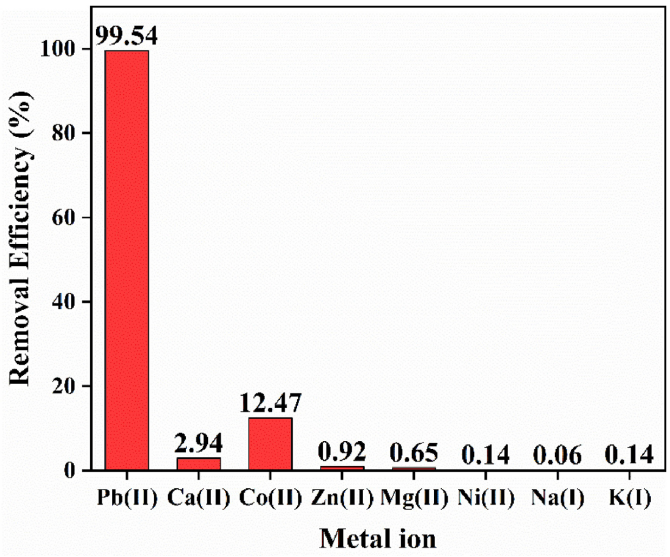

Figure 8. Removal rate of various metal ions in reclaimed water by HNU-G4.

reclaimed water from regenerated water treatment plants. Before and after the adsorption experiment with HUN-G4, the concentrations of various metal ions are shown in Supplementary Table 3, and the experimental data were tested by ICP; the removal rate was calculated using Equation (3). HNU-G4 had an up to 99.54% removal efficiency for Pb(II), but less than 15% of other common metal ions were removed, and the removal of Pb(II) by HNU-G4 was unaffected by the presence of other common metal ions [Figure 8]. The experiment demonstrated that Pb(II) removal with HNU-G4 in medium water was significantly faster than removal of other common metal ions. HNU-G4 was, therefore, employed as an adsorbent to remove Pb(II) from the real samples.

CONCLUSIONS

In summary, a bifunctional gel (HNU-G4) with high sensitivity and selectivity to detect and remove trace amounts of Pb(II) was developed in this work with a minimum detection limit (0.766 ppb) well below the WHO permission. Additionally, the larger the specific surface area, the more adsorption sites on the surface. The fiber structure of HNU-G4 provides a larger specific surface area. Therefore, its adsorption of Pb(II) was allowed to reach 480.00 $mg \cdot g^{-1}$, and the adsorption amount is higher than or comparable to the reported results. After six rounds of detection, adsorption, and regeneration, the gel demonstrated good reusability. Furthermore, it demonstrated good applicability in the Pb(II) detection in real media reclaimed water samples, which has a lot of promise for use in real-world scenarios. This work provides a new design strategy for the detection and adsorption of Pb(II) and suggestions for developing new multifunctional functional materials for monitoring and removing Pb(II) contamination.

DECLARATIONS

Authors' contributions

Designed the experiments, performed data acquisition, writing - original draft preparation, formal analysis: Fang Y

Supervision, investigation, visualization, writing - review and editing: Ren G, Pan Q

Validation, formal analysis: Yu K, Wang C, Zhou Q, Che G, Li M

Availability of data and materials

The detailed materials and methods in the experiment were listed in the Supplementary Materials.

Financial support and sponsorship

This study received funding from several sources, including the National Natural Science Foundation of China (Nos. 22361016 and 22361017), the Natural Science Foundation of Hainan Province (No. 221RC451), the Education Department of Hainan Province (No. Hnky2022ZD-3), the Innovation Platform for Academicians of Hainan Province, and the Specific Research Fund of the Innovation Platform for Academicians of Hainan Province (No. YSPTZX202321), and the International Science & Technology Cooperation Program of Hainan Province (No. GHYF2022006).

Conflicts of interest

All authors declared that there are no conflicts of interest.

Ethical approval and consent to participate

Not applicable.

Consent for publication

Not applicable.

REFERENCES

1. Wang Z, Li TT, Peng HK, Ren HT, Lou CW, Lin JH. Low-cost hydrogel adsorbent enhanced by trihydroxy melamine and β-cyclodextrin for the removal of Pb(II) and Ni(II) in water. *J Hazard Mater* 2021;411:125029. DOI PubMed
2. Jasim SA, Hachem K, Abdelbasset WK, Yasin G, Suksatan W, Chem C. Efficient removal of Pb(II) using modified chitosan Schiff

base@Fe/NiFe. *Int J Biol Macromol* 2022;204:644-51. DOI PubMed
3. Rajput S, Pittman CU Jr, Mohan D. Magnetic magnetite (Fe_3O_4) nanoparticle synthesis and applications for lead (Pb^{2+}) and chromium (Cr^{6+}) removal from water. *J Colloid Interface Sci* 2016;468:334-46. DOI PubMed
4. Ozdes D, Gundogdu A, Kemer B, Duran C, Senturk HB, Soylak M. Removal of Pb(II) ions from aqueous solution by a waste mud from copper mine industry: equilibrium, kinetic and thermodynamic study. *J Hazard Mater* 2009;166:1480-7. DOI PubMed
5. Zhang J, Li L, Li Y, Yang C. Microwave-assisted synthesis of hierarchical mesoporous nano-TiO_2/cellulose composites for rapid adsorption of Pb^{2+}. *Chem Eng J* 2017;313:1132-41. DOI
6. Li G, Ye J, Fang Q, Liu F. Amide-based covalent organic frameworks materials for efficient and recyclable removal of heavy metal lead (II). *Chem Eng J* 2019;370:822-30. DOI
7. Huang Z, Xiong C, Ying L, et al. A post-functional Ti-based MOFs composite for selective removal of Pb (II) from water. *J Hazard Mater* 2022;432:128700. DOI PubMed
8. Wang P, Shen T, Li X, Tang Y, Li Y. Magnetic mesoporous calcium carbonate-based nanocomposites for the removal of toxic Pb(II) and Cd(II) ions from water. *ACS Appl Nano Mater* 2020;3:1272-81. DOI
9. Lu S, Huang J, Liu G, et al. Ammonia-modulated reversible gel-solution phase transition and fluorescence switch for a salicylhydrazide-based metal-organic gel. *RSC Adv* 2017;7:30979-83. DOI
10. Liu W, Yang Y, Zhong Q, et al. Zr^{4+}-based metal organic gel as a fluorescent "Turn on-off" sensing platform for the selective detection and adsorption of CrO_4^{2-}. *Mater Chem Front* 2021;5:1932-41. DOI
11. You D, Shi H, Xi Y, et al. Simultaneous heavy metals removal via in situ construction of multivariate metal-organic gels in actual wastewater and the reutilization for Sb(V) capture. *Chem Eng J* 2020;400:125359. DOI
12. Wang H, Chen BH, Liu DJ. Metal-organic frameworks and metal-organic gels for oxygen electrocatalysis: structural and compositional considerations. *Adv Mater* 2021;33:e2008023. DOI PubMed
13. Gao Y, Liu Z, Li Y, Zou D. Three-in-one multifunctional luminescent metal-organic gels/sodium alginate beads for high-performance adsorption and detection of chlortetracycline hydrochloride, and high-security anti-counterfeiting. *Chem Eng J* 2023;452:139194. DOI
14. Ma Y, Li A, Gao X, et al. Effective separation of enantiomers based on novel chiral hierarchical porous metal-organic gels. *Macromol Rapid Commun* 2019;40:e1800862. DOI PubMed
15. Qi H, Zhang T, Jing C, et al. Metal-organic gel as a fluorescence sensing platform to trace copper(II). *Anal Methods* 2021;14:52-7. DOI PubMed
16. Zhang K, Dai Z, Zhang W, et al. EDTA-based adsorbents for the removal of metal ions in wastewater. *Coord Chem Rev* 2021;434:213809. DOI
17. Huang Z, Zhao M, Wang C, Wang S, Dai L, Zhang L. Preparation of a novel Zn(II)-imidazole framework as an efficient and regenerative adsorbent for Pb, Hg, and As ion removal from water. *ACS Appl Mater Interfaces* 2020;12:41294-302. DOI PubMed
18. Yin N, Wang K, Wang L, Li Z. Amino-functionalized MOFs combining ceramic membrane ultrafiltration for Pb (II) removal. *Chem Eng J* 2016;306:619-28. DOI
19. Kumar A, Chowdhuri AR, Laha D, Mahto TK, Karmakar P, Sahu SK. Green synthesis of carbon dots from *Ocimum sanctum* for effective fluorescent sensing of Pb^{2+} ions and live cell imaging. *Sensor Actuat B Chem* 2017;242:679-86. DOI
20. Varaprasad K, Nùñez D, Ide W, Jayaramudu T, Sadiku ER. Development of high alginate comprised hydrogels for removal of Pb(II) ions. *J Mol Liq* 2020;298:112087. DOI
21. Chen JF, Liu X, Ma JF, et al. A pillar[5]arene-based multiple-stimuli responsive metal-organic gel was constructed for facile removal of mercury ions. *Soft Matter* 2017;13:5214-8. DOI PubMed
22. Chen J, Dong R, Chen S, et al. Selective adsorption towards heavy metal ions on the green synthesized polythiophene/MnO_2 with a synergetic effect. *J Clean Prod* 2022;338:130536. DOI
23. Wang Y, van Zwieten L, Wang H, et al. Sorption of Pb(II) onto biochar is enhanced through co-sorption of dissolved organic matter. *Sci Total Environ* 2022;825:153686. DOI PubMed
24. Fu L, Wang S, Lin G, et al. Post-modification of UiO-66-NH_2 by resorcyl aldehyde for selective removal of Pb(II) in aqueous media. *J Clean Prod* 2019;229:470-9. DOI
25. Ahmadijokani F, Tajahmadi S, Bahi A, et al. Ethylenediamine-functionalized Zr-based MOF for efficient removal of heavy metal ions from water. *Chemosphere* 2021;264:128466. DOI PubMed
26. Saleem H, Rafique U, Davies RP. Investigations on post-synthetically modified UiO-66-NH_2 for the adsorptive removal of heavy metal ions from aqueous solution. *Micropor Mesopor Mater* 2016;221:238-44. DOI
27. Tang J, Chen Y, Zhao M, Wang S, Zhang L. Phenylthiosemicarbazide-functionalized UiO-66-NH_2 as highly efficient adsorbent for the selective removal of lead from aqueous solutions. *J Hazard Mater* 2021;413:125278. DOI PubMed
28. Zhang YW, Cao Y, Mao CJ, Jiang D, Zhu W. An iron(III)-based metal-organic gel-catalyzed dual electrochemiluminescence system for cytosensing and in situ evaluation of the $VEGF_{165}$ subtype. *Anal Chem* 2022;94:4095-102. DOI PubMed
29. Gu D, Yang W, Lin D, et al. Water-stable lanthanide-based metal-organic gel for the detection of organic amines and white-light emission. *J Mater Chem C* 2020;8:13648-54. DOI
30. Fang Y, Ren G, Li M, Yang Y, Guo D, Pan Q. Sensitively liquid and gaseous detection of formaldehyde based on a supramolecular organic framework. *Sensor Actuat B Chem* 2021;349:130726. DOI
31. Sun Y, Dramou P, Song Z, et al. Lanthanide metal doped organic gel as ratiometric fluorescence probe for selective monitoring of ciprofloxacin. *Microchem J* 2022;179:107476. DOI

32. Zhang Y, Li B, Ma H, Zhang L, Zhang W. An RGH-MOF as a naked eye colorimetric fluorescent sensor for picric acid recognition. *J Mater Chem C* 2017;5:4661-9. DOI
33. Afzalinia A, Mirzaee M. Ultrasensitive fluorescent miRNA biosensor based on a "sandwich" oligonucleotide hybridization and fluorescence resonance energy transfer process using an Ln(III)-MOF and Ag nanoparticles for early cancer diagnosis: application of central composite design. *ACS Appl Mater Interfaces* 2020;12:16076-87. DOI PubMed
34. Song XX, Fu H, Wang P, Li HY, Zhang YQ, Wang CC. The selectively fluorescent sensing detection and adsorptive removal of Pb^{2+} with a stable [δ-Mo_8O_{26}]-based hybrid. *J Colloid Interface Sci* 2018;532:598-604. DOI PubMed
35. Wu P, He Y, Lu S, et al. A regenerable ion-imprinted magnetic biocomposite for selective adsorption and detection of Pb^{2+} in aqueous solution. *J Hazard Mater* 2021;408:124410. DOI PubMed
36. Ngana BN, Seumo PMT, Sambang LM, Dedzo GK, Nanseu-njiki CP, Ngameni E. Grafting of reactive dyes onto lignocellulosic material: application for Pb(II) adsorption and electrochemical detection in aqueous solution. *J Environ Chem Eng* 2021;9:104984. DOI
37. Awual MR. Innovative composite material for efficient and highly selective Pb(II) ion capturing from wastewater. *J Mol Liq* 2019;284:502-10. DOI
38. Pei L, Yang H, Chen S, Wang L. UiO-66-NHC(S)NHMe/three-dimensional macroporous carbon for removal and electrochemical detection of Cd^{2+}, Pb^{2+}, Cu^{2+}, and Hg^{2+}. *Ind Eng Chem Res* 2022;61:1588-95. DOI
39. Awual MR, Hasan MM, Iqbal J, et al. Naked-eye lead(II) capturing from contaminated water using innovative large-pore facial composite materials. *Microchem J* 2020;154:104585. DOI
40. Sun Y, Jian-wang, Li P, Yang M, Huang X. Highly sensitive electrochemical detection of Pb(II) based on excellent adsorption and surface Ni(II)/Ni(III) cycle of porous flower-like NiO/rGO nanocomposite. *Sensor Actuat B Chem* 2019;292:136-47. DOI
41. Schecher WD, Mcavoy DC. MINEQL+: a software environment for chemical equilibrium modeling. *Comput EnvironUrban Syst* 1992;16:65-76. DOI
42. Qi N, Zhao H, Qin Y, Wang Q, Wang G, Li Y. An innovative strategy for synchronous treatment of combined heavy metal and organic pollutants through polysaccharide gel encapsulating S^2. *Sci Total Environ* 2020;742:140601. DOI PubMed
43. Ha HD, Jang M, Liu F, Cho Y, Seo TS. Upconversion photoluminescent metal ion sensors via two photon absorption in graphene oxide quantum dots. *Carbon* 2015;81:367-75. DOI
44. Park M, Ha HD, Kim YT, et al. Combination of a sample pretreatment microfluidic device with a photoluminescent graphene oxide quantum dot sensor for trace lead detection. *Anal Chem* 2015;87:10969-75. DOI PubMed